SERVO COMPONENT ANALYSIS, THE FOUNDATION OF AUTOMATIC CONTROL SYSTEM DESIGN

MILTON O. PAUL
AND
BOBBY L. POTTS

SERVO COMPONENT ANALYSIS, THE FOUNDATION OF AUTOMATIC CONTROL SYSTEM DESIGN

* * * * *

Milton O. Paul

and

Bobby L. Potts

SERVO COMPONENT ANALYSIS, THE FOUNDATION OF AUTOMATIC CONTROL SYSTEM DESIGN

by

Milton O. Paul
Lieutenant, United States Navy

and

Bobby L. Potts
Lieutenant, United States Navy

Submitted in partial fulfillment of
the requirements for the degree of

MASTER OF SCIENCE
IN
ELECTRICAL ENGINEERING

United States Naval Postgraduate School
Monterey, California

1 9 5 8

SERVO COMPONENT ANALYSIS, THE FOUNDATION OF AUTOMATIC CONTROL SYSTEM DESIGN

by

Milton O. Paul

and

Bobby L. Potts

This work is accepted as fulfilling
the thesis requirements for the degree of
MASTER OF SCIENCE
IN
ELECTRICAL ENGINEERING
from the
United States Naval Postgraduate School

ABSTRACT[1]

Several techniques are presented for analyzing the servomechanism component and determining the transfer function or describing function plots of the element as a function of frequency. An original method to measure the transfer function of a "d-c component" is developed.

The basis of the analysis is the "frequency response method," that is, to excite a unit under test with a sinusoidal signal at a number of fixed frequencies covering the interested frequency range. A constant input signal amplitude is used and the output amplitude and phase angle of the fundamental wave in the Fourier frequency spectrum is noted in each instance. These results are put into proper form and recorded on the Bode, the Nichols, or the Nyquist diagram. From this information, the stability of the system and the transfer function of the device can be closely approximated.

One of the techniques described was implemented at the Electrical Engineering Laboratory of the United States Naval Postgraduate School, Monterey, California. The device was utilized to test a Kay Lab notch filter. The experimental results were substantiated by the analytical data.

[1]The authors with to express their gratitude to Dr. W. A. Stein, Dr. G. J. Thaler, and Prof. W. C. Smith, all of the United States Naval Postgraduate School, and to Walter Sterling of Convair Corporation for their encouragement and assistance in the preparation of this thesis. We also wish to thank A. J. White for the construction of the mechanical portion of the experimental equipment.

TABLE OF CONTENTS

LIST OF ILLUSTRATIONS

TABLE OF SYMBOLS AND ABBREVIATIONS

a-c	Alternating Current
cps	Cycles per Second
db	Decibel
d-c	Direct Current
emf	Electromotive Force
K	Proportionality Constant
kcps	Kilocycles per Second
min	Minimum
rms	Root Mean Square
s	Laplace Transform Variable
ω_c	Carrier Frequency (radians per second)
ω_d	Data Frequency (radians per second)
ω_l	Lower Side-Band Frequency (radians per second)
ω_u	Upper Side-Band Frequency (radians per second)

1. Introduction

The component analysis of the automatic control system offers a great challenge to the electrical engineer. The utilization of the analog and digital computers for design of servo systems has greatly aided the engineer in producing an acceptable automatic control system. However, the problem of establishing the transfer function of the basic control system element is still a formidable one and unless this mathematical description of the components is accurate and exact, the engineer has no assurance that the manufactured system will perform its function according to design predictions. Whatever the field of application, the designer is, in almost every case, faced with the same basic problem - providing the stiffest possible control over the working frequency range consistent with freedom from oscillation or under-damped response. Such design work demands a full knowledge of the transfer function of each element employed in the control loop.

This problem, the determination of an accurate transfer function or describing function plot, is the basic topic for the authors' investigation.

First, it is necessary to describe briefly the servo component and the design requirements placed upon the component.

The basic components of a control system are:

1. A prime power source to furnish energy to the

output load.

2. A controlling device for the prime power source.
3. A measuring device to record and transmit the output variable.
4. An error detector which accepts the input signal, compares the input to the output, and provides an error signal to remove the difference between the input command and the output response. The error signal is then fed to the controlling device forming a closed loop system.

Two important performance requirements are placed on the servo control system components. The first requirement is stability. When a feedback control loop exists it is possible for any component to transmit an excess of energy to the succeeding unit so that the response to a given disturbance produces an error signal, the amplitude of which increases indefinitely with time. The above describes an unstable system. If the response to a given disturbance produces an error signal which approaches a constant value, the system is stable. If the system response produces an oscillatory error signal, and the amplitude of the oscillation approaches a constant value, the system is conditionally stable. In most applications, the design engineer wishes to produce an automatic control system which is absolutely stable. If the system is unstable, it must be adjusted or compensated, or the components causing the instability must be replaced.

The second performance requirement is the accuracy with

which the component transmits the command signal to the succeeding unit to exert dynamic control over the specific load in accordance with the command. This constitutes an error analysis. Because the automatic control system is a dynamic system, the error is usually described with a differential equation for linear systems and with a describing function for nonlinear systems. The solution for the differential equation may be divided into two parts, the transient or general solution, and the steady state or particular solution. Therefore system performance logically has two divisions, steady state performance and transient performance. Steady state performance is usually described in terms of position error, velocity error, etc.; transient performance may be specified in terms of speed of response, settling time, peak overshoot, transient oscillation frequency, damping ratio, etc.

Design specifications in terms of the above parameters are usually based on operational requirements. Before the design engineer can select his basic components, he must have a thorough knowledge of the time domain specifications and the frequency domain specifications. Usually the specifications are set forth in figures of merit. Some of these are:

1. Damping factor
2. Damping ratio
3. Settling time

4. Peak overshoot

5. Rise time

6. Bandwidth

7. Delay time

After the formulation of design specifications based on the above performance characteristics, the choice of basic units for the servo system is influenced by:

1. The physical nature of load, which imposes power and energy requirements on the drive motor. Transient power requirements dictate the size of the motor and current capacity. The acceleration characteristics of the motor are also of prime importance.
2. The nature of the controlling device for the driver. For example, the amplidyne generator of an amplidyne-motor combination must have sufficient power to meet all field requirements of the motor.
3. The type of measuring device needed to record and transmit load position, load velocity, load acceleration, etc.
4. The type of data input device to accept the command signal.
5. The type of error detector needed to compare the command signal with the output and provide an error signal.

6. A means of operating the controller from the error signal.

All components of the system must be selected in accordance with:

1. The power capacity and the power requirements for each device.
2. The physical suitability of each device. The size, shape, weight, temperature tolerance, tolerance to acceleration, environmental conditions to which the device will be exposed -- all are of prime importance in the choice of the unit.
3. The accuracy with which the device performs its assigned function.
4. The reliability of the device. Reliability must be built into each component of the servo system.

With the above as a guide, the designer obtains a basic servo system which is physically capable of doing the task required. The system has sufficient power capacity, measurements are sufficiently accurate, and corrective power is applied to reduce the error toward zero. It does not follow, however, that the basic system would perform satisfactorily if assembled and tested.

The design of an automatic control system results in a device which is characterized by definite performance features in both the time and frequency domains. There are many ways

to compute f(t) from F(ω),[1] but in higher order systems the amount of labor involved is exhorbitant. For this reason, the professional leaders in the field of industrial engineering turn to the analog or digital computer to synthesize the control system and obtain an accurate transient response. Compensation to meet specifications is done on a trial and error basis.

No matter what the method of design, the system equation of motion must be accurate. Correlation is needed in both directions, from the frequency domain function, F(ω), to the time domain function, f(t), and from the time domain function to the frequency domain function. These two functions are related by the direct Fourier transformation and the inverse Fourier transformation (Fourier integral), and any method of correlation must necessarily approximate these integrations.

Several design requirements have not been considered. The speed of response and the steady state position error have not been used explicitly in selecting components. Even if the speed of response for individual components has been investigated, and components chosen accordingly, it is very unlikely that the desired transient performance will be met

[1](a) H. M. James, N. B. Nichols, R. S. Phillips, Theory of Servo Mechanisms, McGraw-Hill Book Co., Inc., New York, 1947, pp. 43-50.
(b) G. S. Brown, D. P. Campbell, Principles of Servomechanisms, John Wiley & Sons, Inc., New York, 1948, pp. 332-350.
(c) D. V. Stallard, A Series Method of Calculating Control-System Transient Response from the Frequency Response, Transactions AIEE, 1955.

using the combination of these components with a feedback path around them.

The next step in design is to determine what performance characteristics might be expected from the proposed servo system without actually building and testing it.

The accurate construction of a mathematical model is not an easy task and usually requires linear approximations for devices which are not linear throughout the entire operating range. Also, many simplifying assumptions must be made to arrive at a differential equation or describing function for which a solution can be obtained. At best, the solutions obtained from these equations are indicative of the basic system performance, but are not exact unless the mathematical model is a perfect representation of the actual system. To determine accurately the transfer function plot of the servo component is of great importance and is the foundation of control system design. Once the transfer function plot is established, the mathematical description of the component may be obtained readily by utilizing existing frequency response methods.

Whatever the method of system design, the precision with which the final product performs reflects the accuracy of "component analysis."

2. The Solartron Equipment

One device which does an excellent job of transfer function analysis is the Solartron equipment manufactured by Solartron Laboratory Instruments, Ltd., Thames Ditton, Surrey, England.

The Solartron equipment consists of three units. The first is a low frequency decade oscillator for generating a four-phase reference signal of ten volts rms with a frequency range of .01 cps to 11.1 kcps.

The second unit is the phase-sensitive voltmeter which accepts the reference signals from the oscillator and the output signal from the device under test. Two six-inch scale-length meters are provided; the function of these is to indicate separately, in terms of true voltage, the resolved components of the signal input which are in phase and in quadrature with the reference input voltage. This resolved component presentation permits direct plotting of a Nyquist diagram on ordinary linear graph paper, thus eliminating the need for polar coordinate paper. The phase-sensitive voltmeter has a frequency 0.5 cps to 1 kcps.

An important feature of the phase-sensitive voltmeter is that the meter indications are to a first order, independent of harmonic or spurious frequency content in the signal voltage, providing that the reference voltage employed is itself free from such imperfections.

The third unit is the Solarscope, which is a precision oscilloscope for the observation of the reference and signal

voltages.

The principal device in the Solartron equipment which makes signal phase and amplitude measurement possible is the phase-sensitive voltmeter. A brief description of its principle of operation follows:

Two thermocouple type wattmeters are employed as shown in Fig. 1. For the purpose of initial explanation, these will be considered as conventional coil type dynamometer wattmeters. The voltage coil of the first meter is fed with the amplified reference voltage, and the voltage coil of the second meter is fed with a quadrature voltage of identical amplitude. Both current coils are fed with current which is in phase with the applied signal voltage.

The moving coil of wattmeter one will, at any instant, be subject to a torque which is proportional to the product of the voltage and current present in the appropriate coils.

The components are, in turn, proportional to the applied reference and signal components respectively, hence the ultimate indication of the wattmeter may be written:

$$\text{Indication} = \frac{K}{t}\int_0^t V_r \cdot V_s \, dt \qquad (1)$$

where V_r is the reference voltage,

V_s is the signal voltage,

K is a constant,

t is time (long compared with either periodic time.)

If V_r is of the form sin t, the above integral over long term will be zero for all forms of V_s other than $V_s = A \sin(\omega t + \phi)$

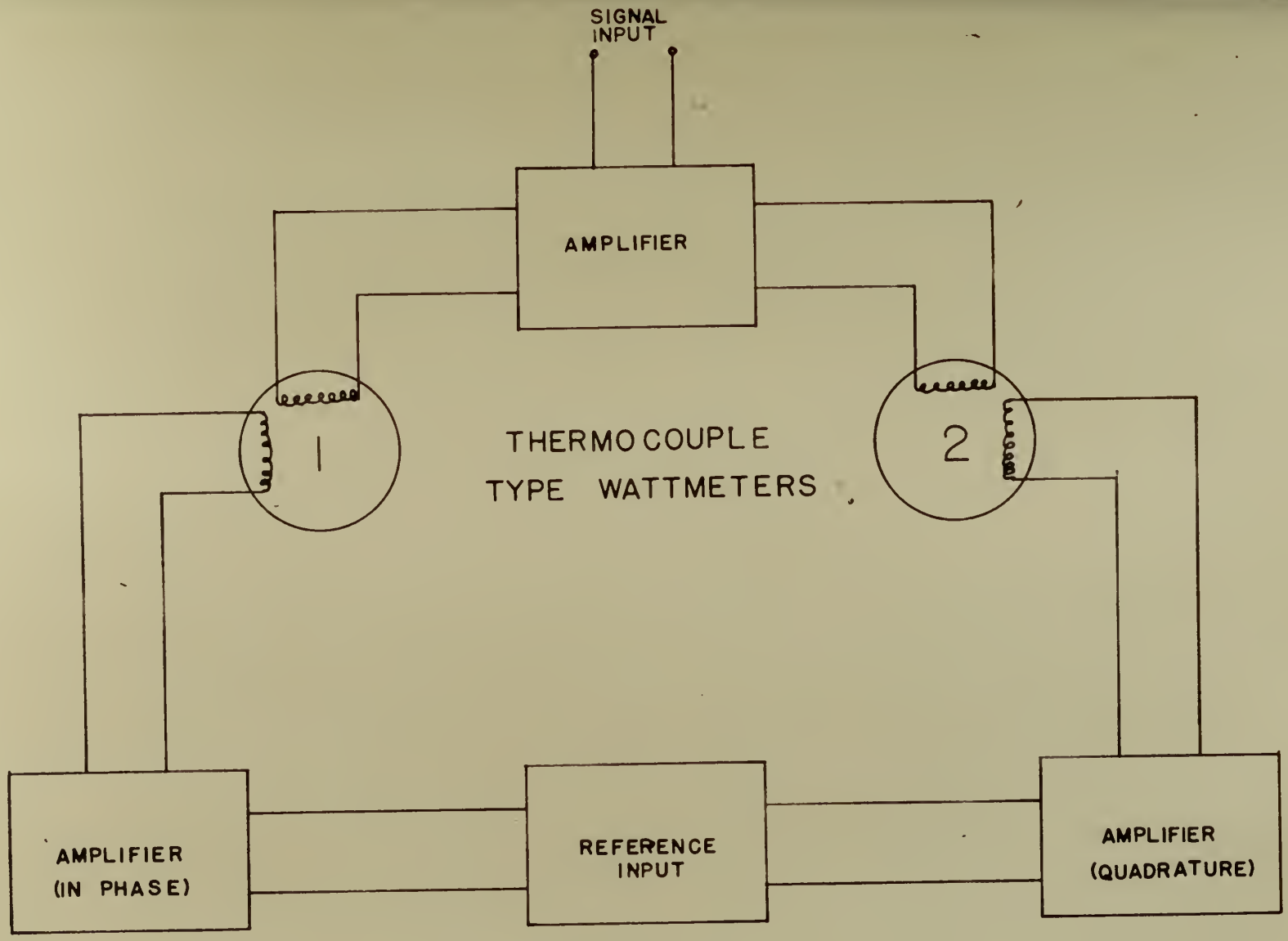
SIGNAL
INPUT
AMPLIFIER
1
THERMOCOUPLE
TYPE WATTMETERS
2
AMPLIFIER
(IN PHASE)
REFERENCE
INPUT
AMPLIFIER
(QUADRATURE)

FIGURE 1

where A is a constant. Hence, when a reference voltage of sine wave form is used, the meter will not respond to quadrature, harmonic or unrelated frequencies in the signal voltage. Further, if the reference voltage is maintained at constant value, the indication will be directly proportional to the component of the signal voltage, which is in phase with the reference voltage.

Wattmeter two, shown in Fig. 1, has its voltage coil supplied at 90° phase shift to the reference voltage; consequently, it will respond only to the quadrature component of the signal input.

Conventional coil type dynamometer wattmeters have the following disadvantages as regards phase-sensitive voltmeters:

1. Require substantial energizing power
2. Restricted frequency range
3. Rather bulky and unwieldy

The low frequency phase-sensitive voltmeter, therefore, employs thermocouple type wattmeters which, in addition to being six-inch scale panel mounting instruments, have a greatly reduced power consumption. The meters are sensitive to frequencies of 0.5 cps to 1 kcps.

Fig. 2 illustrates in block diagram form the various component circuits which together constitute the phase-sensitive voltmeter.

The whole system is concerned with feeding the two indicating meters with the correct electrical quantities. It is, therefore, necessary at this stage to examine the

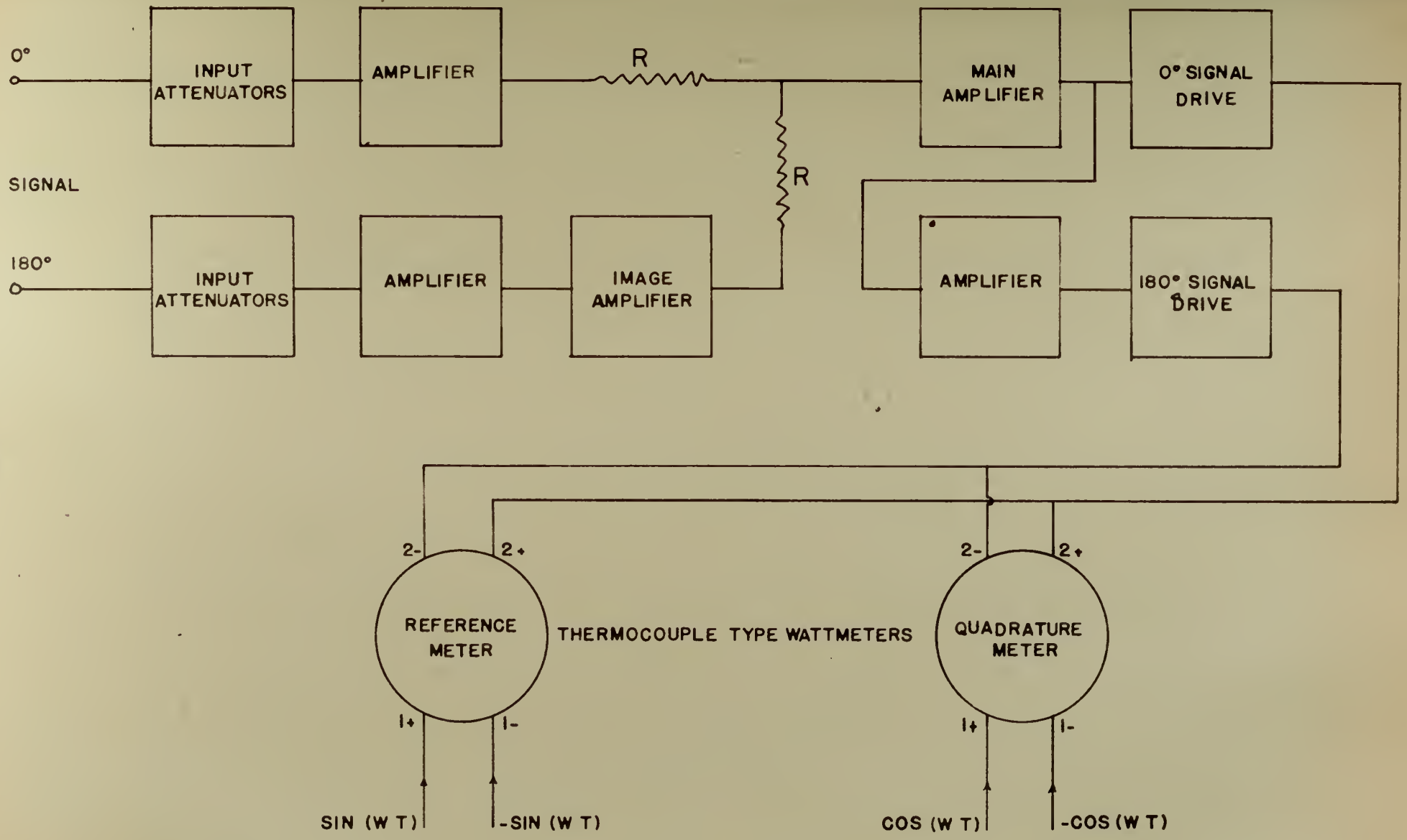

PHASE SENSITIVE VOLTMETER

FIGURE 2

meters in more detail. This examination, however, will be confined to requirements and sensitivity, and will not consider functional technique.

The thermocouple wattmeter in this application should be considered as a current rather than a power measuring device. This conception is grasped readily by visualizing a conventional d-c wattmeter fed with a constant voltage at the voltage coil. Such an arrangement would then constitute a d-c milliammeter as viewed from the current coil terminals. Applying this concept to the meters shown in Fig. 3, they are designed for a constant current of ten milliamperes fed through terminals 1+ and 1- and, when so energized, they have a current sensitivity of five milliamperes full scale as viewed from terminals 2+ and 2-.

The function of the 0° and 180° reference drive amplfiers is to supply a balanced drive current of ten milliamperes through terminals 1+ and 1- of the reference meter for a nominal input of ten volts per phase. Similarly, the 90° and 270° reference drive provides quadrature energization for the quadrature meter.

The input attenuator has two identical sections, one for each input channel. It is a ladder attenuator of one megohm resistance and provides half-decade steps (10 db. approximately), and is arranged so that the voltage presented to the input amplifier is less than 50 millivolts. When the instrument is used to measure unbalanced signals,

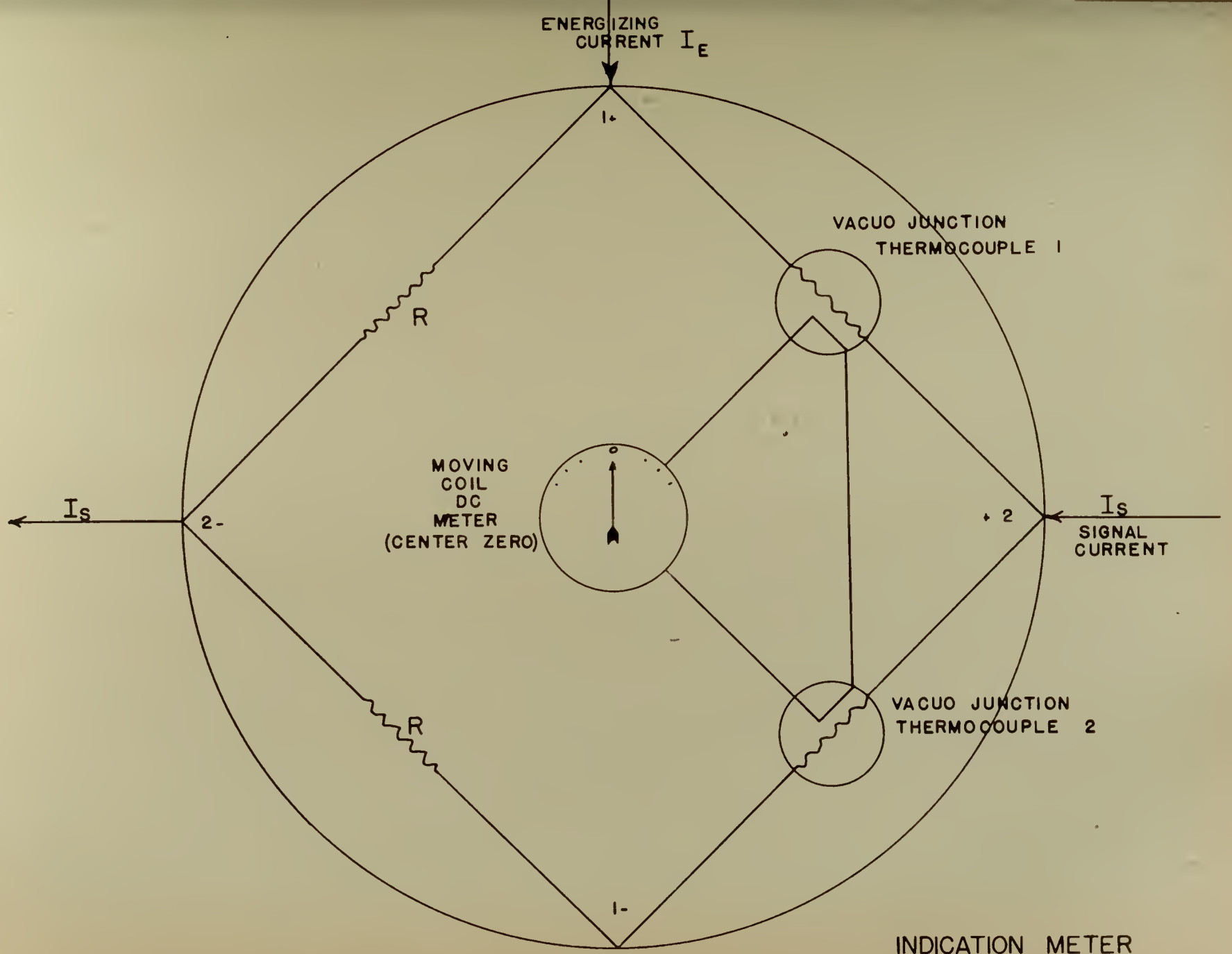
ENERGIZING CURRENT I_E
1+
VACUO JUNCTION THERMOCOUPLE 1
R
MOVING COIL DC METER (CENTER ZERO)
I_S
2-
+ 2
I_S
SIGNAL CURRENT
R
VACUO JUNCTION THERMOCOUPLE 2
1-
INDICATION METER

FIGURE 3

the 180° input system is shorted out by a switch.

The input amplifiers are identical, and each has a fixed voltage gain of approximately 17. The 180° input amplifier is followed by an image amplifier which is purely a phase inverter. When a balanced signal is applied, the output of the 180° input system is added to that of the 0° input system in the resistor, R, adding chain. The net result is that the indication for a balanced input of x volts per phase is twice that for an unbalanced input of x volts.

The main amplifier has a preset voltage gain of approximately 20.

Image amplifier two provides phase inversion which feeds the 180° signal drive amplifier. The two signal drive amplifiers provide balanced drive which will deliver five milliamperes into terminals 2+ and 2- of both reference and quadrature meters; i.e., full scale for either meter, depending on the phase of the input signal.

The blocking time constants used in the signal system are a compromise between bulk and permissible phase shift in the instrument. To compensate for phase shift in the signal channel due to these components, the blocking time constant used in the reference amplifiers is arranged to give an approximate equivalent phase shift. The net overall error is negligible in the working frequency range of the instrument.

The response of the system will be examined now in more detail for the application of alternating currents.

It will be assumed that the thermocouple emf is propor-

tional to the average heating effect, hence:

$$e = K_1 \int i^2 \qquad (2)$$

where e = thermocouple emf

K_1 is a constant

i = instantaneous heater current

The meter indication, which is proportional to the difference of the thermocouple emf's, may therefore be written:

$$\text{Indication} = K_2 (e_2 - e_1) \qquad (3)$$

where e_1 and e_2 are the emf's of the corresponding thermocouples

K_2 is a constant.

Substituting from above, this may be expressed:

$$\text{Indication} = K(\int i_2^2 - \int i_1^2) \ldots \qquad (4)$$

From Fig. 3: $i_2 = \frac{1}{2} I_E + I_S \qquad (5)$

and $i_2^2 = \frac{1}{4}(I_E^2 + I_S^2 + 2I_E I_S)$

Similarly: $i_1^2 = \frac{1}{4}(I_E^2 + I_S^2 - 2 I_E I_S) \qquad (6)$

Substituting in (3) above,

$$\text{Indication} = \frac{K_3}{4} (\int I_E^2 + \int I_S^2 + 2\int I_E I_S - \int I_E^2 - \int I_S^2 + 2\int I_E I_S) \qquad (7)$$

$$= K_3 \int I_E I_S$$

Equation (7) is the basic equation of response for a watt-meter.

The voltage and current requirements for the instrument

are met by a hard tube regulated power supply which delivers approximately 180 milliamperes and has an a-c source impedance of less than one ohm over the working frequency range. A low voltage rail at 70 volts is also required at low source impedance. This is obtained by means of a further stabilizing system operating directly from the 250 volt rail.

3. A Synchro Device to Analyze a "d-c Component"

The actuating signal information present in the servo-loop is usually in the form of a voltage, either modulated direct voltage or modulated alternating voltage. In the case of the former, the servo system components respond to an error signal, whose polarity determines the direction of motion, and the magnitude of the signal determines the amount of force applied to the load. This type of component is called a "d-c component."

To analyze the "d-c component" by a frequency response method, a sinusoidal generator is needed to excite the unit under test with frequencies varying from zero to infinity. Because the servo system is essentially a low pass filter, sinusoidal excitation above 60 cps is rarely required. The amplitude of the excitation voltage should be a constant value of the same order of magnitude as the unit requires under normal operating conditions.

To complete the analysis, a device is needed to measure the attenuation and phase shift of the input signal caused by the component under test. If the results of this test (phase shift and attenuation ratio) are plotted on the Bode diagram, the transfer function of the component can be obtained.[1]

Fig. 4 shows the basic elements of a synchro device

[1] G. J. Thaler, Servomechanism Theory, McGraw-Hill Book Co., Inc., New York, 1955, pp. 77-96

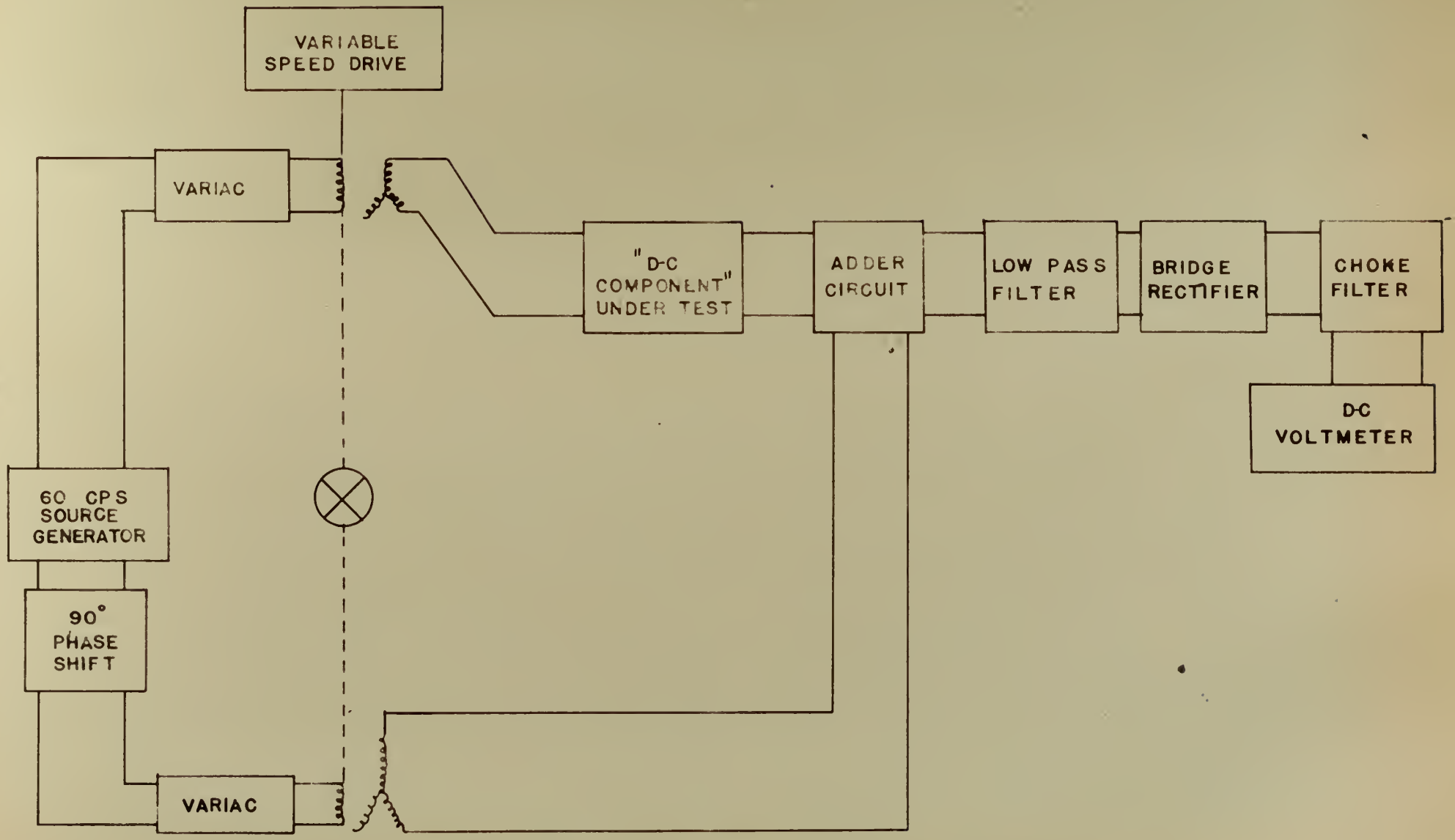

A SYNCHRO DEVICE TO ANALYZE A "D-C COMPONENT"

FIGURE 4

designed by the authors which will measure the phase shift and attenuation of a "d-c component" for frequencies from zero+ to 50 cps. Isolating amplifiers to remove loading effects are omitted for simplicity and clarity of explanation.

The equipment consists of two control transformers driven by a variable speed drive. The rotors are mechanically connected through a differential so that they turn at the same speed and that a phase displacement may be made in the stator output voltages. The rotors are excited externally from a single sinusoidal generator with a carrier frequency. The carrier frequency may be any value. However, considering the inertia forces in the mechanical parts, 60 cps seems to be a logical choice.

Both rotors are driven at the various discrete test frequencies so as to produce a voltage in the stators of the form:

$$v_1 = K \sin \omega_c t \sin \omega t \tag{8}$$

where ω is angular frequency of rotation

ω_c is the carrier frequency

$K = 1$.

Through the use of trigonometric identities, the above equation can be written.

$$v_1 = \tfrac{1}{2} \cos(\omega_c - \omega)t - \tfrac{1}{2} \cos(\omega_c + \omega)t \tag{9}$$

$$= \tfrac{1}{2} \cos \omega_l t - \tfrac{1}{2} \cos \omega_u t$$

This equation shows that the voltage v_1 is the sum of

two voltages, one of the lower side-band frequency $\omega_l = \omega_c - \omega$, and one of the upper side-band frequency $\omega_u = \omega_c + \omega$. Because the carrier frequency is not present in this signal, this form of voltage is known as "suppressed carrier modulation."

If the above voltages are made inputs to a "d-c component," the component will modify each side band voltage, introducing an attenuation factor, G, and a phase shift, ϕ. Using the superposition theorem and adding the separate components of the output voltages, the output reduces to:

$$v_{01} = \tfrac{1}{2} G_l \cos(\omega_l t + \phi_l) - \tfrac{1}{2} G_u \cos(\omega_u t + \phi_u) \qquad (10)$$

By shifting the carrier frequency to the second control transformer by 90° and displacing the rotor mechanical position 90° from reference rotor, the stator voltage of the second control transformer is of the form:

$$\begin{aligned} v_2 &= \cos\omega_c t \cos\omega t \qquad (11) \\ &= \tfrac{1}{2}\cos(\omega_c+\omega)t + \tfrac{1}{2}\cos(\omega_c-\omega)t \\ &= \tfrac{1}{2}\cos\omega_u t + \tfrac{1}{2}\cos\omega_l t \end{aligned}$$

Adding equations (9) and (11) removes the lower side-band and only the upper side-band is left:

$$v_1 + v_2 = \cos\omega_u t \qquad (12)$$

It is upon this principle that the device is proposed. Because the output voltages of the "d-c component" are attenuated and shifted in phase, the output voltage of the second control transformer must be similarly attenuated and phase-shifted so that the lower side-band will be eliminated. This is accomplished easily by attenuating the carrier input to the second control transformer and by turning the differential

between the two rotors, introducing a phase shift, ϕ_2.

$$v_2 = G_2 \cos \omega_c t \cos(\omega t - \phi_2) \qquad (13)$$
$$= \tfrac{1}{2} G_2 \cos[(\omega_c + \omega)t - \phi_2]$$
$$+ \tfrac{1}{2} G_2 \cos[(\omega_c - \omega)t + \phi_2]$$

If G_2 is made equal to G_1 and ϕ_2 is made equal to ϕ_1, by adding equations (10) and (13), the lower side-band is eliminated.

The physical method of adding the above equations involves the use of an operational amplifier of the variety so extensively used in analog computations. After adding the two signals, the upper side-band is removed by a low pass filter and a bridge rectifier is placed on the output of the filter.

If a d-c voltmeter is placed across the rectifier circuit, a minimum signal will be read when the two lower side-bands are in phase. This is accomplished physically by turning the differential until the d-c voltmeter indicates a minimum. Now the amplitude of the carrier to the second control transformer is raised or lowered through the variac until the d-c voltmeter nulls. A comparison of this amplitude with the reference carrier amplitude specifies the attenuation ratio and the phase shift is proportional to the angle through which the differential was turned to minimize the reading.

In the previous discussion, no mention was made of the magnitude of rotor rotation. A simple illustration using

equation (9) follows:

To excite a "d-c component" with a 1 cps sinusoidal signal, the lower side-band must equal 1 cps. Therefore with

ω_c = 60 cps (carrier frequency)

ω = 59 cps (rotor rotational velocity)

$$v_{10} = \tfrac{1}{2} \cos 2\pi(60+59)t - \tfrac{1}{2} \cos 2\pi(60-59)t \qquad (9)$$
$$= \tfrac{1}{2} \cos 2\pi(119)t - \tfrac{1}{2} \cos 2\pi(1)t.$$

With the results of phase shift and attenuation ratio as a function of frequency, the "d-c component" may be analyzed utilizing the Bode, Nichols or Nyquist plots.

4. A Synchro Device to Analyze an "a-c Component"

The analysis of the components of an alternating current servomechanism is inherently more difficult than that of the direct current servomechanism. In the alternating current system, the actuating signal or error voltage is an amplitude-modulated alternating voltage of the form

$$v = K \epsilon \sin \omega_c t \tag{14}$$

where ϵ = error

K = sensitivity of the component (volts per unit of error)

ω_c = carrier frequency

The two-phase motor is a good example of an "a-c component." If a modulated alternating voltage is applied to the motor, the magnitude of the restoring torque is determined by the magnitude of the error voltage, and the direction is determined by whether the phase of the error voltage is in phase with or 180° out of phase with a reference voltage.

To analyze the "a-c component" by frequency response methods, a suppressed carrier signal of the form

$$v = K \sin\omega_c t \sin \omega t \tag{15}$$
$$= \tfrac{1}{2} \cos(\omega_c - \omega)t - \tfrac{1}{2} \cos(\omega_c + \omega)t$$

where $K = 1$

needs to be generated. The generated signal is then made the input to the component under test and the angular frequency, ω, is varied in discrete steps from zero to infinity.

Because the servo control system is essentially a low pass filter, the upper limit of frequency variation is normally ω = 60 cps.

Equation (15) shows that the suppressed carrier signal is made up of the sum of two voltages, $\frac{1}{2}\cos(\omega_c - \omega)t$, the lower side-band, and $\frac{1}{2}\cos(\omega_c + \omega)t$, the upper side-band. Each of these side-band voltages is operated upon by the component under test, resulting in a phase shift and attenuation to the suppressed carrier input.

Fig. 5 shows the basic elements of a synchro device which will measure the phase shift and attenuation of an "a-c component" for frequencies of zero+ to 30 cps. Isolating amplifiers to remove loading effects are omitted for clarity of explanation.

The equipment consists of the following basic elements:

1. A 400 cycle frequency generator.
2. A control transformer driven by a variable speed drive to generate the suppressed carrier signal voltage.
3. A second control transformer to modulate the phase-shifted and attenuated suppressed carrier output signal from the unit under test.
4. A mechanical differential between the rotors of the control transformers to resolve and measure phase shift introduced by the component under test.
5. A demodulator to obtain a d-c voltage proportional to the envelope of the modulated signal.

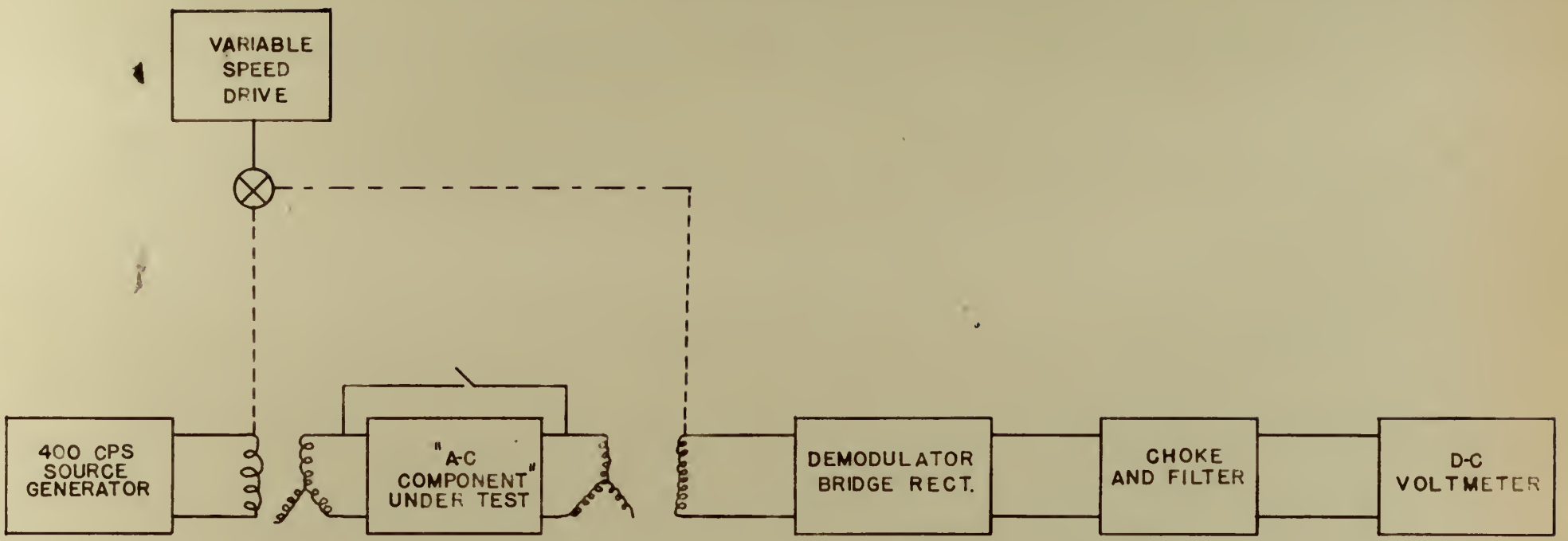

A SYNCHRO DEVICE TO ANALYZE AN "A-C COMPONENT"

FIGURE 5

6. A filter to remove all the a-c components in the demodulated signal.

7. A d-c voltmeter to integrate and record the relative signal levels.

A theoretical analysis of the circuit shown in Fig. 5 establishes the basic principles for operation.

A sinusoidal carrier signal of constant amplitude is supplied to the rotor of the first control transformer. By rotating the rotor at the desired data frequency, a suppressed carrier signal of the form

$$v_1 = \sin(\omega_c t) \sin \omega_d t \qquad (16)$$

is generated in the stator windings of the control transformer. The above expression can be written in terms of the upper and lower side-band frequencies, but the mathematical explanation is more clearly defined if the equation is left in the above form.

The suppressed carrier signal is now applied to the "a-c component" under test and is attenuated and phase-shifted. Because the 400 cps carrier frequency is not actually utilized in the "a-c component," an assumption is made that the phase shift is introduced in the $\sin \omega_d t$ term only. (This assumption will be proven valid in the experimental section.) Therefore the output of the "a-c component" is

$$v_0 = |G| \sin \omega_c t \sin(\omega_d t + \phi) \qquad (17)$$

where $|G|$ is the attenuation of the signal

ϕ is phase shift.

By modulating the above signal with the rotation of the

second rotor at the same frequency, ω_d, the expression becomes

$$v_{OR2} = \sin \omega_c t \sin(\omega_d t + \phi) \quad [\sin \omega_d t] \tag{18}$$

The mechanical differential placed between the two rotors allows a phase shift to be introduced at the second rotor. By turning the differential an amount ϕ, or $\phi + 90^\circ$, equation (18) becomes

$$v_{OR2} = \sin \omega_c t \sin^2 \omega_d t \tag{19}$$

$$\text{or} \quad v_{OR2} = \sin \omega_c t \sin \omega_d t \cos \omega_d t \tag{20}$$

respectively.

Next the above signals are demodulated with a full wave bridge rectifier and filtered to remove harmonic content. This leaves a signal proportional to the envelope of equations (19) and (20) and has the form

$$v = \sin^2 \omega_d t \tag{21}$$

$$\text{or} \quad v = \sin \omega_d t \cos \omega_d t = \tfrac{1}{2} \sin 2 \omega_d t \tag{22}$$

The d-c voltmeter averages or integrates these signals, producing a maximum reading when the second rotor position produces a $\sin^2 \omega_d t$ voltage and a minimum reading when the second rotor position produces a $\frac{1}{2} \sin 2 \omega_d t$ voltage. Through the integration process the higher harmonics are eliminated according to the relationship

$$v_{d-c} = \int \sin m \omega_d t \sin n \omega_d t = 0 \tag{23}$$

for integral values of $m \neq n$

By adjusting the differential until the d-c voltmeter reads a maximum for a given rotational data frequency, ω_d, the out-

put amplitude and phase angle of the fundamental wave in the Fourier frequency spectrum can be obtained. Comparing these values with the reference values obtained when the "a-c component" was removed from the circuit gives the required amplitude and phase versus frequency data for the transfer function plot.

5. Analyzing the Kay Lab Notch Filter, an "a-c Component"

The Kay Lab notch filter is essentially a parallel T filter network with a by-pass channel. Fig. 6 shows the circuit construction. Sometimes the parallel T filter is called a derivative network, for it provides stabilization for the a-c servo system.[1] Essentially, it performs the function which a lead network performs for the d-c servomechanism. The parallel T filter operates on a suppressed carrier signal, which is composed of the upper and lower side-band voltages.

$$v = \cos \omega_c t \cos \omega_d t \qquad (24)$$
$$= \tfrac{1}{2} \cos(\omega_c + \omega_d)t + \tfrac{1}{2} \cos(\omega_c - \omega_d)t$$

Rewriting the above in terms of the carrier frequency only

$$v = \tfrac{1}{2} \cos(1 + \delta)\, \omega_c t + \tfrac{1}{2} \cos(1 - \delta)\, \omega_c t \qquad (25)$$

where $\delta = \frac{\omega_d}{\omega_c}$

To produce a lead network transfer function of the form

$$G(s) = (1 + s\tau_d) \qquad (26)$$

where τ_d = time constant of the circuit,

it is necessary to have in addition to the input error signal, $\cos \delta\omega_c t$, a derivative of the input error signal

$$\frac{d}{dt} \cos \delta\omega_c t = - \delta\omega_c \sin \delta\omega_c t \qquad (27)$$

[1] G. M. Attura, Effects of Carrier Shifts on Derivative Networks for a-c Servomechanisms, AIEE Technical Paper 51-100, December, 1950, pp. 1-4.

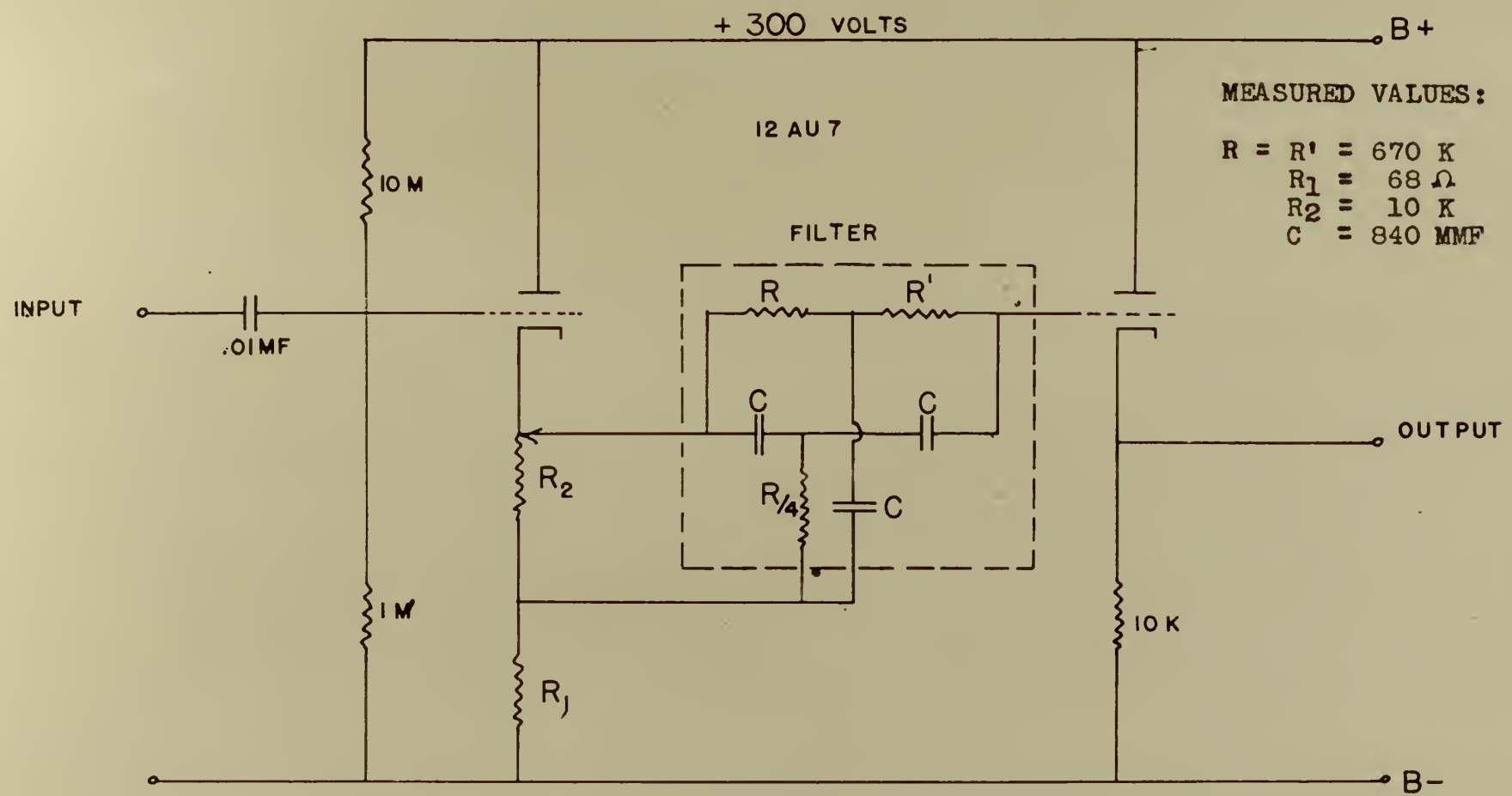

KAY-LAB NOTCH FILTER

FIGURE 6

Therefore the error signal required to be the output of the parallel T filter is the carrier signal times the sum of the input signal and the derivative signal

$$v_0 = \cos \delta\omega_c t \ [\cos \omega_c t] - \tau_d \delta\omega_c \sin \delta\omega_c t \ [\cos \omega_c t] \quad (28)$$

Since the first term of the above equation is input to the parallel T filter, the filter operates on this signal and supplies the modulated derivative signal

$$v_{OF} = -\tau_d \delta\omega_c \sin \delta\omega_c t \ [\cos \omega_c t] \quad (29)$$

$$= \tau_d \delta\omega_c \cos(\delta\omega_c t + 90^\circ) \ [\cos \omega_c t] \quad (30)$$

$$= \frac{\tau_d}{2} \delta\omega_c \{\cos[(1+\delta)\omega_c t + 90^\circ] + \cos[(1-\delta)\omega_c t - 90^\circ]\} \quad (31)$$

Thus the parallel T filter is required to advance 90° the phase of the upper side-band and retard 90° the phase of the lower side-band. Furthermore, the magnitudes of the side-band signals should be proportional to $\delta\omega_c$, the data frequency. Fig. 7 graphically shows the phase shift and attenuation characteristics of the network.

To show that the parallel T filter in the Kay Lab notch filter effectively supplies a derivative signal, the transfer function is derived as follows:

First, Bartlett's Bisectional Theorem[1] is applied to determine the impedance of the network. The theorem requires

[1] E. A. Guilleman, Communication Circuits, Volume II, John Wiley & Sons, Inc., New York, 1935, pp. 439.

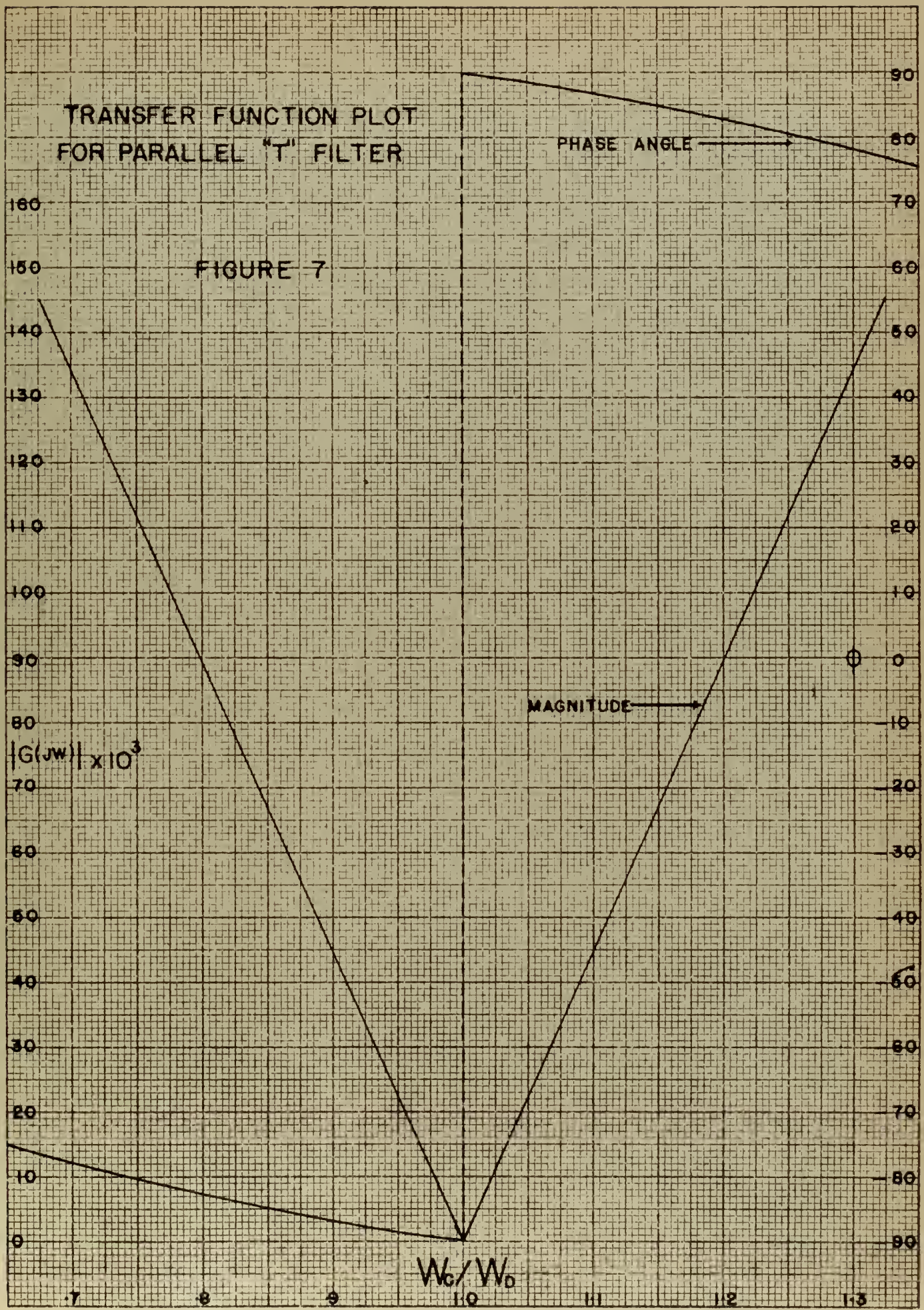
TRANSFER FUNCTION PLOT
FOR PARALLEL "T" FILTER
FIGURE 7
PHASE ANGLE
MAGNITUDE
|G(JW)| x 10^3
Wc/Wo
160
150
140
130
120
110
100
90
80
70
60
50
40
30
20
10
0
90
80
70
60
50
40
30
20
10
0
10
20
30
40
50
60
70
80
90
.7
.8
.9
1.0
1.1
1.2
1.3

that the network be bisected so that the circuit is identical on each side of the bisector line. Refering to Fig. 6, the parallel T network will be symmetrical if the R/4 resistor is made a parallel combination of two R/2 resistors and the capacitance, C_3, is made a parallel combination of two $C_{3/2}$ capacitors. Fig. 8 shows this evolution and the bisected half of the circuit.

The next step in the application of this theorem is to label any bisected portions of the circuit. This establishes points A and B of Fig. 8.

The third step is to determine the short circuit impedance of the bisected network by connecting points A and B to ground.

$$(s) = \frac{R \times 1/sC}{R + 1/sC} = \frac{R/sC}{(RsC + 1)/sC} = \frac{R}{RsC + 1} \qquad (32)$$

The fourth step is to determine the open circuit impedance of the bisected network by leaving points A and B open-circuited.

$$= \frac{(R + 2/sC) \times (R/2 + 1/sC)}{(R + 2/sC) + (R/2 + 1/sC)} \qquad (33)$$

$$= \frac{RsC + 2}{sC}$$

After the impedances Z_{SC} and Z_{OC} have been found, the parallel T filter is replaced by a lattice shown in Fig. 9.

BISECTED PARALLEL "T" FILTER

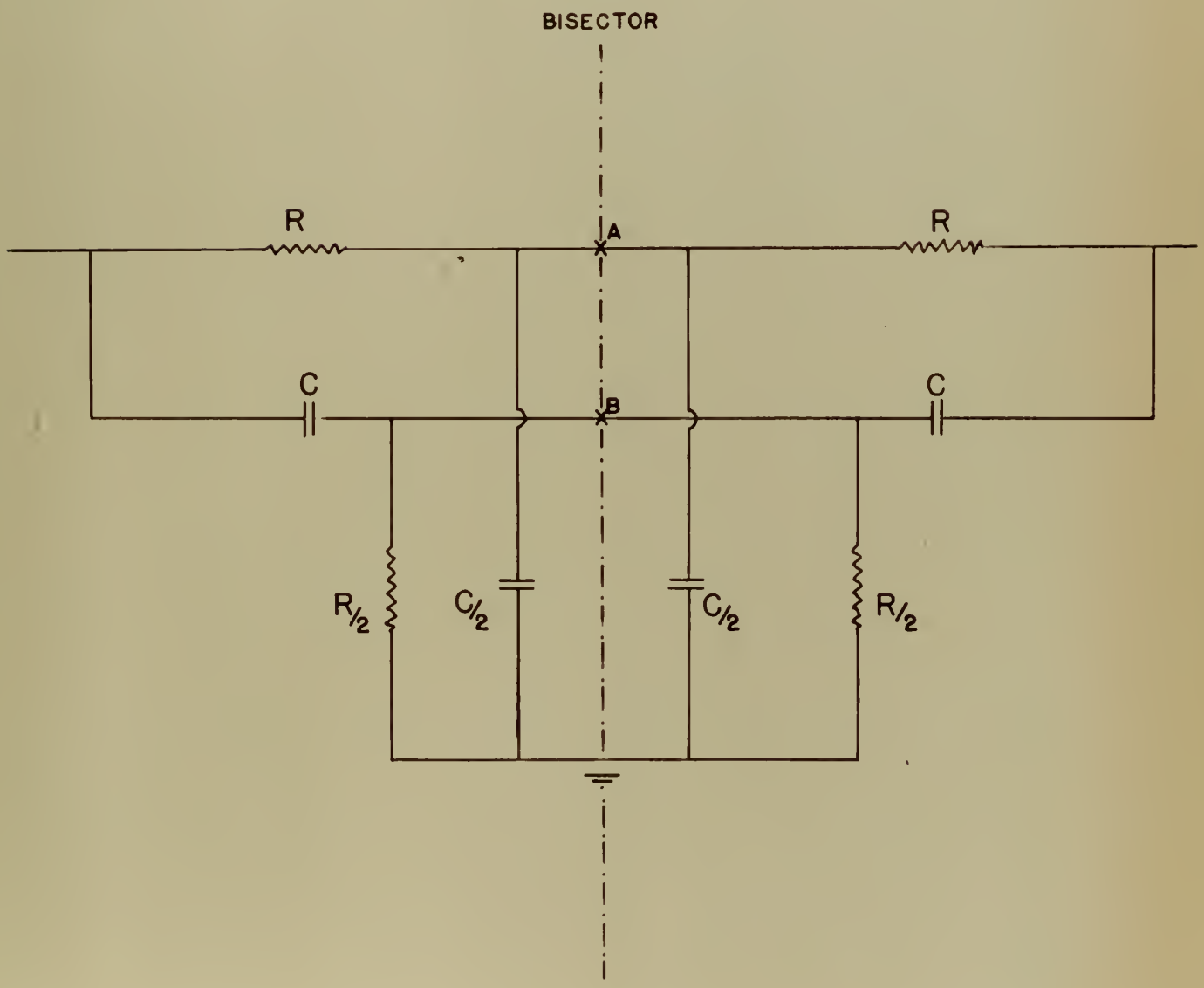

FIGURE 8

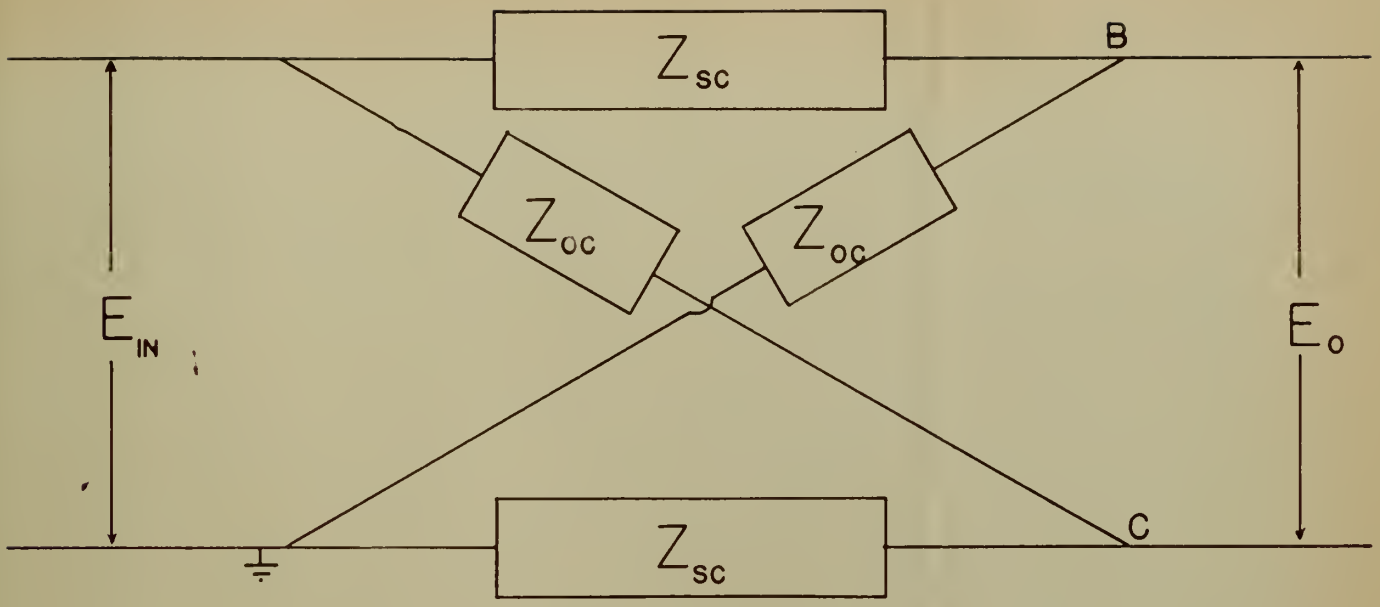

LATTICE NETWORK STRUCTURE FOR
PARALLEL "T" FILTER

FIGURE 9

Providing that $E_0 = V_{BC}$ is fed to the grid of a tube so that I_1 and I_2 are the only currents flowing,

$$\frac{E_0}{E_{IN}}(s) = \frac{Z_{OC} - Z_{SC}}{Z_{OC} + Z_{SC}} = \frac{R_S C + 2}{(RsC)^2 + 6RsC + 2} \qquad (34)$$

(For derivation of the above formula using the lattice structure of Fig. 9, see Appenix I.)

Dividing through by $(RsC)^2 + 2$ and replacing s by $j\omega$,

$$\frac{E_0}{E_{IN}} = \frac{1}{1 - \frac{j\,6\,RC\omega}{(RC\omega)^2 - 2}} \qquad (35)$$

A plot of the above function, using the parameters of the Kay Lab notch filter, is shown on Fig. 7, and the re-

quirements to advance and retard the phase of the upper and lower side-bands respectively are fulfilled. Furthermore, the magnitudes of the side-band signals are proportional to the data frequency.

The previous discussion applies to the parallel T filter only. The Kay Lab notch filter described in Fig. 6 has a bypass channel. This bypass is essentially a potential divider and allows a certain portion of the input error signal to bypass the filter. The bypassed signal combines vectorially with the output of the parallel T filter, broadens the notch, removes the discontinuity in phase shift at the carrier frequency, and produces a real term proportional to the error itself.[1]

The transfer function of the parallel T filter with bypass (neglecting loading effects) is

$$\frac{V_O}{V_{IN}} = \frac{R_1}{R_1 + R_2} + \frac{R_2}{R_1 + R_2} \left[\frac{E_O}{E_{IN}}\right] \tag{36}$$

$$\frac{V_O}{V_{IN}} = \frac{R_1}{R_1 + R_2} + \frac{R_2}{R_1 + R_2} \left[\frac{1}{1 - \frac{j\,6\,RC\omega}{(RC\omega)^2 - 2}}\right] \tag{37}$$

Fig. 10 shows the plot of this function (amplitude and phase angle versus frequency) for the notch filter used in the experimental analysis described in the next section.

Although formula (37) is the exact transfer function of the notch filter with bypass channel for frequencies above or below the carrier, it does not describe adequately the

[1] G. M. Attura, op. cit., p. 2

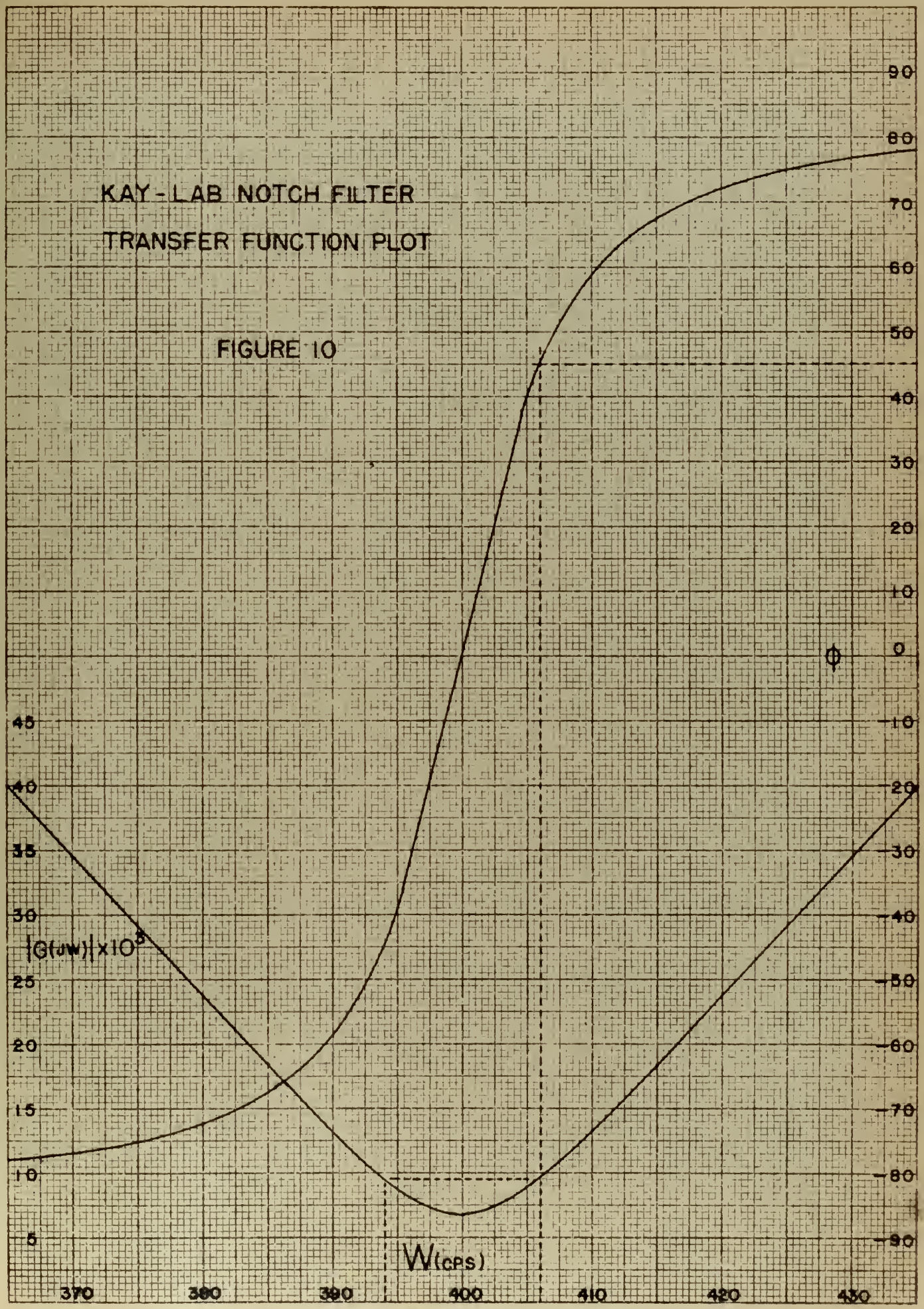
KAY-LAB NOTCH FILTER
TRANSFER FUNCTION PLOT
FIGURE 10
90
80
70
60
50
40
30
20
10
0
-10
-20
-30
-40
-50
-60
-70
-80
-90
Φ
45
40
35
30
25
20
15
10
5
|G(jw)| x10^3
W(CPS)
370
380
390
400
410
420
430

transfer function of the notch filter based on the data frequency, $\omega_d = (\omega - \omega_c)$. Although equation (26) represents the ideal transfer function of the derivative network, the experimental network transfer function can be represented better by the empirical formula

$$G(j\omega_d) = \frac{\tau_{lag}}{\tau_{lead}} \frac{(1 + j\omega_d \tau_{lead})}{(1 + j\omega_d \tau_{lag})} \qquad (38)$$

When $\omega = \omega_c$, $\omega_d = 0$, the complex terms, $(j\omega_d)$, equal zero and

$$\left|\frac{V_O}{V_{IN}}\right|_{\omega_d=0} = \left|G(j\omega)\right|_{\omega_d=0} = \frac{\tau_{lag}}{\tau_{lead}} \qquad (39)$$

Because the parallel T filter completely rejects the carrier frequency signal, only a small portion of the input signal goes through the notch filter via the bypass channel.

Therefore, at $\omega_d = 0$, $\left|\frac{V_O}{V_{IN}}\right|$ is a minimum and a small number.

Because $\tau_{lead} >> \tau_{lag}$, the denominator in equation (37) is approximately one when $\omega_d = \frac{1}{\tau_{lead}}$. The numerator becomes $\sqrt{2}$ min $\left|\frac{V_O}{V_{IN}}\right|$, which defines the double power points and the notch interval.

$$\text{Notch interval} = \omega_2 - \omega_1 \qquad (40)$$

where $\omega_1 = \omega_\ell - \omega_c$

$\omega_2 = \omega_u - \omega_c$

The notch interval divided by two defines the corner

frequency, (ω_1), for the Bode diagram.

$$\frac{\text{Notch Interval}}{2} = \frac{1}{\tau_{lead}} = \omega_1 \qquad (41)$$

Thus, τ_{lag} and τ_{lead} are specified from equations (39) and (41) when minimum $\left|\frac{V_O}{V_{IN}}\right|$ and the notch interval are known.

Fig. 11 shows the theoretical Bode diagram for the Kay Lab notch filter described in Fig. 6. Appendix II shows the mathematical procedures used to construct this diagram.

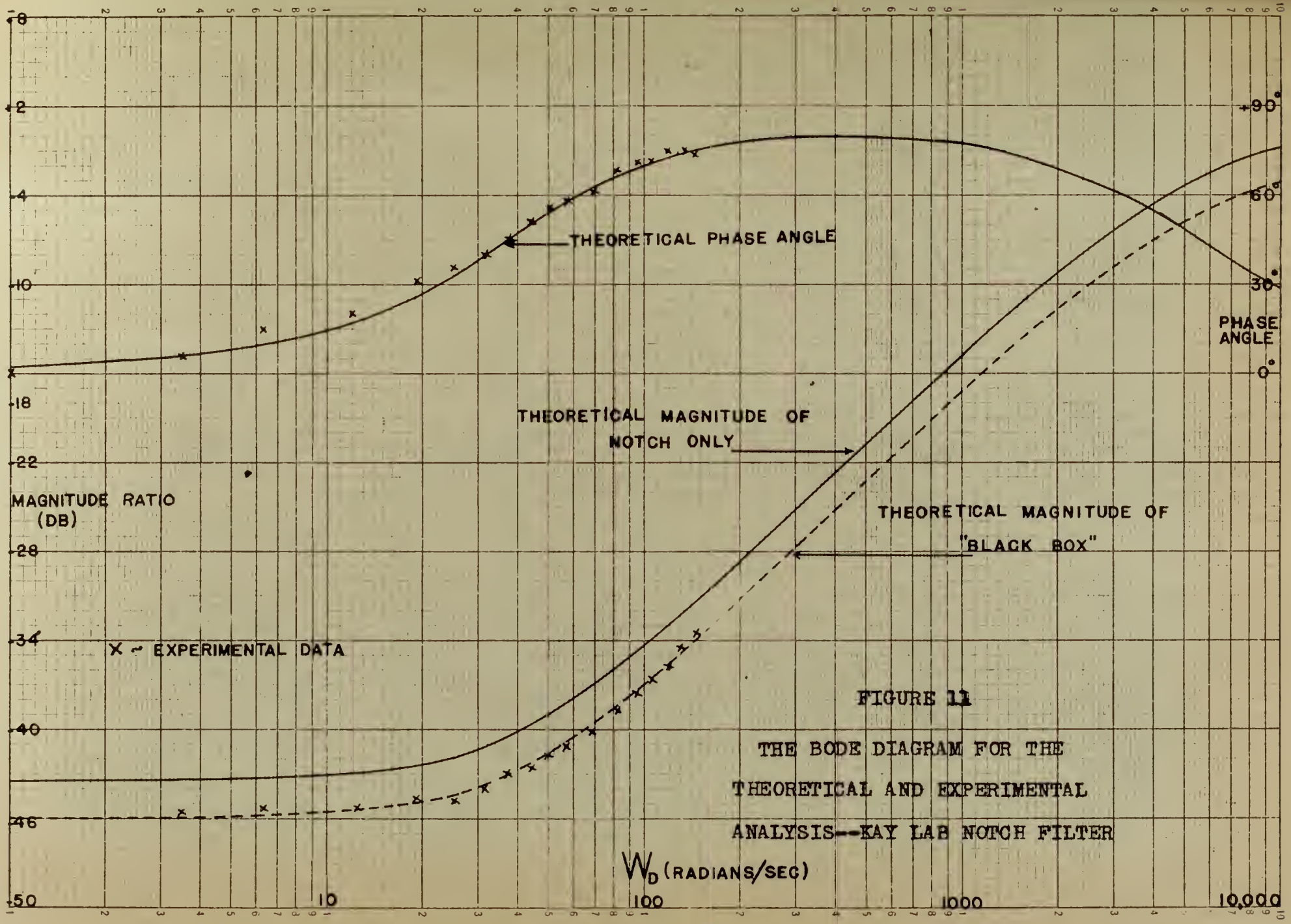

FIGURE 11

THE BODE DIAGRAM FOR THE THEORETICAL AND EXPERIMENTAL ANALYSIS--KAY LAB NOTCH FILTER

6. Experimental Analysis of the Kay Lab Notch Filter

The basic theory, equipment, and procedure for the analysis of an "a-c component" were proposed in Section 4. Section 5 discussed the Kay Lab notch filter in detail, deriving its theoretical transfer function. This section presents the actual experimental evaluation of the Kay Lab notch filter transfer function, using equipment designed and built by the authors.

6.1. Experimental Equipment

Fig. 12 shows in detail the circuit design to produce a working model of the device described in Section 4 for analyzing an "a-c component."

A Hewlett-Packard low frequency generator supplied the 400 cycle carrier signal to the rotor of control transformer #1. By rotating this rotor at various angular speeds from 1.0 radian/sec to 180 radians/sec, a modulated alternating voltage (suppressed carrier) of the form

$$v = K \sin \omega_c t \sin \omega_d t \qquad (42)$$

is produced in the stator windings of the control transformer #1. The #3 stator terminal is grounded and the suppressed carrier signal from #1 stator terminal is fed to the grid of an RCA 5692 triode. This tube amplifies the signal and drives a 6AR6 cathode follower. The cathode follower circuit is a power source for a UTC A-19 audio transformer which reproduces the test signal and isolates the "a-c component" under test.

In this manner, the device under test is isolated from

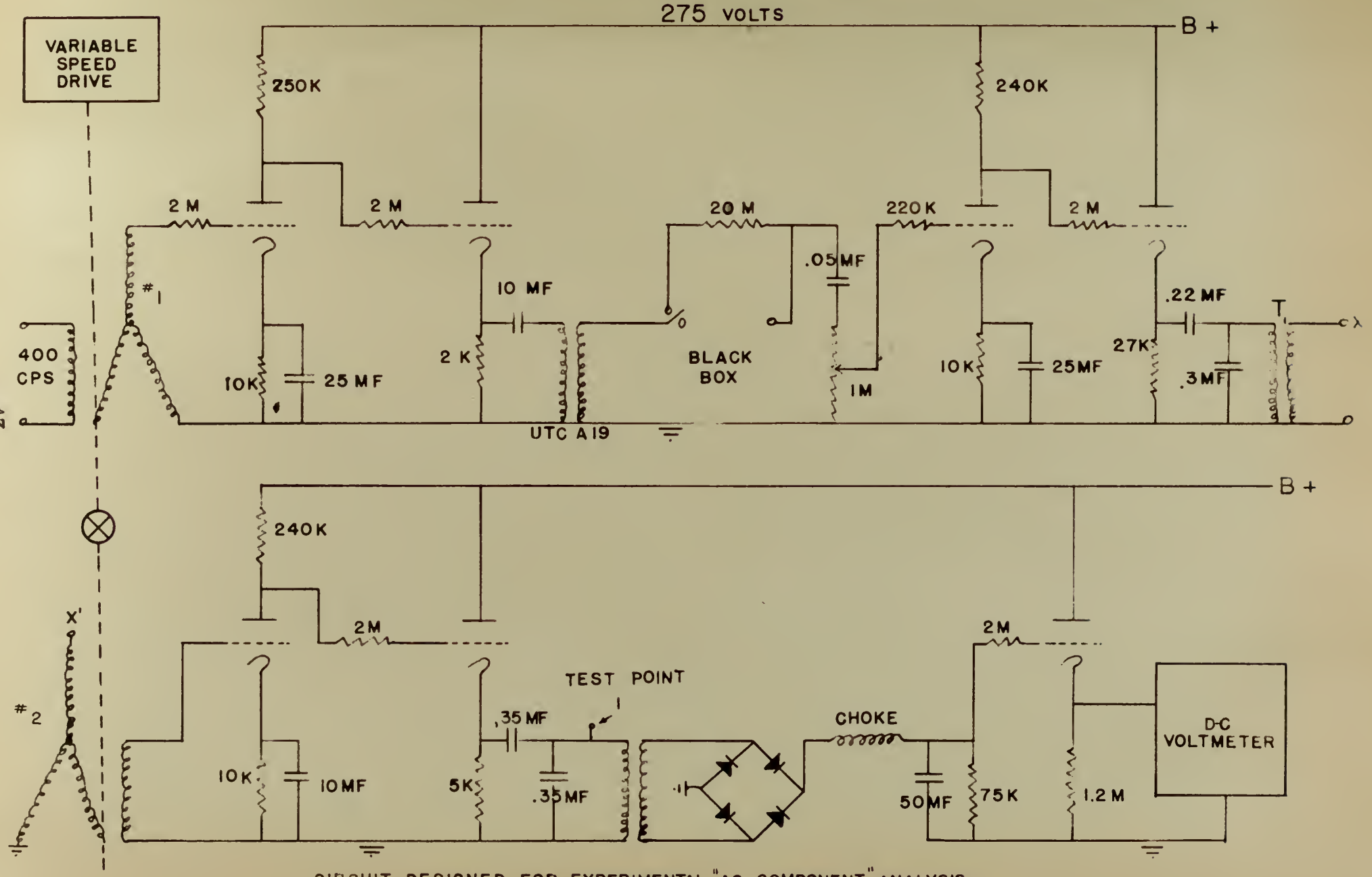

CIRCUIT DESIGNED FOR EXPERIMENTAL "AC COMPONENT" ANALYSIS

FIGURE 12

the control transformer and the control transformer operates into an infinite impedance. A minimum of distortion is introduced in the amplification because of the small grid swing and the low level signal required. A 0.4 volt signal from the 400 cycle generator produces a 24 volt signal as input to the "a-c component" or "black box" as it is sometimes called.

A bypass circuit around the black box is provided to establish a reference magnitude and phase angle measurement. In testing the Kay Lab notch filter, it was necessary to place a 20 megohm resistor in this bypass channel to attenuate the input signal by a known factor without introducing any phase shift. This was necessary in order to have a convenient scale reading on the d-c voltmeter.

On the output side of the black box is a one megohm potentiometer so that the amount of signal voltage applied to the grid of the following amplifier may be controlled. This control allows the optimum scale choice on the d-c voltmeter and prevents distortion to the output signal by limiting the amplifier to "Class A" operation.

The output signal amplifier is one-half of an RCA 5692 twin triode and drives a cathode follower which is the power source for the stator of control transformer #2. To isolate this stator from d-c potential it was necessary to place a transformer between the cathode follower and the stator.

Because of the expected low level of signals and the importance of avoiding phase shift with frequency changes, a geophysical type transformer was used in this critical

portion of the circuit. Design specifications for the transformer required less than 0.1 degree phase shift from 300 to 500 cps. Later tests confirmed that this requirement was met.

The rotor of control transformer #2 is rotated at the same frequency, ω_d, as the rotor of control transformer #1. These two rotors are driven through a mechanical differential which allows a phase shift to be introduced into the system by the angular displacement of the second rotor (control transformer #2) with respect to the first rotor (control transformer #1.)

The output signal of the rotor (control transformer #2) is amplified and sent to a bridge rectifier via a cathode follower and transformer similar to the isolating circuit described previously.

The bridge rectifier, which is composed of four SM 255-739 silicon diodes, performs a full wave rectification and feeds a choke and low pass filter to remove any alternating current ripple introduced by the rectification. This filter circuit also removed any harmonics which might be introduced by the black box or any nonlinear elements in the circuit. The output of the filter is amplified and made input to a d-c voltmeter (TS-34A) from which the integrated value of $|G|_{max}$ is obtained.

6.2. Experimental Procedure

To analyze the Kay Lab notch filter and obtain the experimental transfer function plot, the following procedure

was used: (See Fig. 12).

1. The carrier frequency was set at 400 cps.
2. The rotor of control transformer #1 was statically aligned to the position which allowed maximum amplitude signals to be transmitted to the stator.
3. The rotor of control transformer #2 was aligned to the position for maximum signal transmission by rotating the phase angle input control of the differential.
4. The carrier amplitude was adjusted to produce an input signal to the black box of 20 volts, peak to peak (7.07 volts rms).
5. The bypass switch around the black box was closed.
6. The grid potentiometer following the bypass switch was adjusted to produce a d-c voltmeter reading of 78 volts.
7. The signal wave shape was observed on an oscilloscope at test point #1. Any signal distortion was removed by adjusting the grid potentiometer.
8. The grid of the triode amplifier following the black box was grounded to obtain the d-c zero reference voltage. The voltage observed was 17 volts rms.
9. An angular velocity of ω_d = 0.628 radians/sec was set on the Vickers variable speed drive using a precision tachometer to measure the velocity. The

phase angle control of the differential was adjusted to produce a maximum d-c voltage reading on the d-c voltmeter and the zero phase angle reference was established and recorded. The data frequency, ω_d, was varied from 0.628 radians/sec to 132 radians/sec and there was no phase shift or attenuation introduced by the measuring device. The d-c voltage with the black box bypassed was 56 volts rms.

10. The bypass channel switch was opened and the Kay Lab notch filter was placed in the circuit.
11. The black box (Kay Lab notch filter) was excited with suppressed carrier modulation. The data frequencies, ω_d, were varied in discrete steps from 3.46 radians/sec to 132 radians/sec.
12. At each discrete frequency the d-c voltmeter reading was maximized by adjusting the phase angle differential control. The phase angle to produce the maximum d-c voltage, and the magnitude of the voltage were recorded and are shown in Table 1.
13. The data contained in Table 1 was converted to the coordinates of the Bode diagram and plotted on Fig. 11.

6.3. Experimental Results

The experimental results validate the mathematical analysis of the device proposed in Section 4. The experimental transfer function plot of the Kay Lab notch filter closely approximates the theoretical transfer function plot

TABLE I

Experimental Data for the Analysis of the Kay Lab Notch Filter

Data Frequency radians/sec ω_d	Bypass Channel d-c v $\lvert G\rvert$	Bypass Channel d-c v $\lvert G\rvert_{corr.}$*	Bypass Channel deg $\phi_{corr.}$**	Filter In d-c v $\lvert G\rvert$	Filter In d-c v $\lvert G\rvert_{corr.}$*	Filter In deg ϕ	Filter In deg $\phi_{corr.}$**	Magnitude Ratio # db
0.94	56	39	0	21.3	4.3	0	0	-45.6
3.96	56	39	0	21.3	4.3	4.0	6.0	-45.6
6.28	56	39	0	21.5	4.5	10.0	15.0	-45.2
12.56	56	39	0	21.4	4.4	13.0	19.5	-45.3
19.20	56	39	0	21.8	4.8	22.0	33.0	-44.7
25.20	56	39	0	21.7	4.7	24.0	36.0	-44.9
31.45	56	39	0	22.2	5.2	27.0	40.5	-44.0
37.70	56	39	0	22.8	5.8	30.0	45.0	-43.0
44.20	56	39	0	23.0	6.0	35.0	52.5	-42.7
50.30	56	39	0	23.6	6.6	38.0	57.0	-41.9
56.60	56	39	0	24.0	7.0	39.0	58.5	-41.3
69.20	56	39	0	25.0	8.0	41.0	61.5	-40.1
81.70	56	39	0	26.2	9.2	45.5	68.3	-38.8
94.70	56	39	0	27.5	10.5	48.0	72.0	-37.8
107.00	56	39	0	29.0	12.0	48.5	72.5	-36.6
119.50	56	39	0	30.1	13.1	51.0	76.5	-35.9
132.00	56	39	0	32.1	15.1	50.0	75.0	-34.7

*The d-c meter zero reference voltage is 17 volts.

$\therefore \lvert G\rvert - 17 = \lvert G\rvert_{corr.}$

**In the control transformer 120 mechanical degrees equal 180 electrical degrees.

$\therefore \frac{180}{120}\phi = \phi_{corr.}$

#The 20 megohm resistor in the bypass channel attenuates the signal voltage by a factor of 21 times.

$$\therefore \text{Magnitude Ratio} = \frac{\lvert G\rvert_{corr.\ Filter}}{\lvert G\rvert_{corr.\ Bypass}} \times 21$$

of the black box. The maximum phase angle error is five degrees and the maximum error of magnitude ratio is 0.5 db.

Fig. 11 shows the theoretical Bode diagram for the parallel T notch filter with bypass channel and the theoretical Bode diagram for the Kay Lab notch filter including the isolating cathode followers contained in the filter. Superimposed on this figure are the experimental values of phase shift and magnitude ratio obtained from the synchro device for "a-c component analysis."

The difference between the two theoretical magnitude ratio curves is the product of the individual cathode follower gains, -2.47 db. (See Appendix III for mathematical calculations).

Because of the "goodness of fit" between the theoretical and experimental Bode plots over the range of frequencies investigated, the transfer function of the Kay Lab notch filter is assumed to be

$$G(j\omega_d) = A_{CF} \frac{\tau_{lag}}{\tau_{lead}} \frac{(1 + j\omega_d \tau_{lead})}{(1 + j\omega_d \tau_{lag})} \qquad (43)$$

where A_{CF} = gain product of the cathode followers = 0.75

$\tau_{lead} = 2.655 \times 10^{-2}$ sec

$\tau_{lag} = 1.79 \times 10^{-4}$ sec

which agrees with the empirical formula, equation (38), multiplied by the gain product of the cathode followers.

7. Conclusions

Although the procedures and techniques for design of an automatic control system have advanced tremendously during the past ten years with the advent of the analog and digital computers, the fundamental problem, "component analysis," still remains the key to optimum design. Final control system performance is directly a function of the accuracy with which the servo component is mathematically described.

The investigations contained in this paper have clearly indicated:

1. The synchro control transformer is an excellent vehicle for servo component analysis.
2. The synchro device to analyze an "a-c component" which was designed and built by the authors, effectively measured the phase shift and attenuation characteristics of the Kay Lab notch filter.
3. The synchro device to analyze an "a-c component" can be used to measure the describing function of nonlinear elements. The device measures the amplitude and phase angle of the first harmonic of the system output with respect to a sinusoidal input.
4. By precision design utilizing the principles stated in Sections 3 and 4, a single device could be manufactured to produce transfer function plots accurate to one degree of phase shift and 0.1 db magnitude ratio for "a-c and d-c components."

BIBLIOGRAPHY

1. R. Oldenburger, Frequency Response, ASME Publication, The Macmillan Co., New York, 1956.

2. H. M. James, N. B. Nichols, R. S. Phillips, Theory of Servomechanisms, McGraw-Hill Book Co., Inc., New York, 1947.

3. G. S. Brown, D. P. Campbell, Principles of Servomechanisms, John Wiley & Sons, Inc., New York, 1948.

4. G. J. Thaler, Servomechanism Theory, McGraw-Hill Book Co., Inc., New York, 1955.

5. G. M. Attura, Effects of Carrier Shifts on Derivative Networks for a-c Servomechanisms, AIEE Technical Paper 51-100, December, 1950.

6. E. A. Guillman, Communication Circuits, Volume II, John Wiley & Sons, Inc., New York, 1935.

7. D. K. Gehmlich, M. E. Van Valkenburg, Measurement of Some Nonlinearities in Servomechanisms, AIEE Applications and Industry, No. 15, November, 1954.

APPENDIX I

Refering to Fig. 9, the transfer function of the parallel T filter is derived as follows:

$$V_B = I_1 Z_{oc} = \left[\frac{E_{IN}}{Z_{sc} + Z_{oc}}\right] Z_{oc}$$

$$V_c = I_2 Z_{sc} = \left[\frac{E_{IN}}{Z_{oc} + Z_{sc}}\right] Z_{sc}$$

$$V_{BC} = V_B - V_c = E_o = \left[\frac{E_{IN}}{Z_{oc} + Z_{sc}}\right] \left[Z_{oc} - Z_{sc}\right]$$

$$\therefore \quad \frac{E_o(s)}{E_{IN}} = \frac{Z_{oc} - Z_{sc}}{Z_{oc} + Z_{sc}} = \frac{\frac{1}{3}\left[\frac{RsC+2}{sC}\right] - \left[\frac{R}{RsC+1}\right]}{\frac{1}{3}\left[\frac{RsC+2}{sC}\right] + \left[\frac{R}{RsC+1}\right]}$$

$$= \frac{[RsC+1][RsC+2] - 3RsC}{[RsC+1][RsC+2] + 3RsC}$$

$$= \frac{RsC+2}{[RsC]^2 + 6RsC + 2}$$

APPENDIX II

Mathematical Calculations for the Construction of Fig. 11.

(a) The Parallel T Notch Filter with Bypass Channel (from Fig. 10):

$$\text{Min} = \left|\frac{V_O}{V_{IN}}\right| = \frac{\tau_{lag}}{\tau_{lead}} = 6.75 \times 10^{-3} \qquad (39)$$

$$\text{Notch Interval} = \frac{2}{\tau_{lead}} = 75.4 \text{ radians/sec} \qquad (41)$$

Solving equation (41) for τ_{lead}:

$$\tau_{lead} = \frac{2}{75.4} = 2.655 \times 10^{-2} \text{ sec}$$

Substituting the above value in equation (39):

$$\tau_{lag} = \tau_{lead} \left|\frac{V_O}{V_{IN}}\right|_{min} = (2.655 \times 10^{-2})(6.75 \times 10^{-3})$$

$$= 1.79 \times 10^{-4} \text{ sec}$$

$$\therefore \quad G(j\omega_d) = \frac{\tau_{lag}}{\tau_{lead}} \frac{1 + j\omega_d \tau_{lead}}{1 + j\omega_d \tau_{lag}} \qquad (38)$$

$$= 6.75 \times 10^{-3} \left[\frac{1 + j\omega_d 2.655 \times 10^{-2}}{1 + j\omega_d 1.79 \times 10^{-4}}\right]$$

A plot of the above equation for values of ω_d from 1 to 500 radians/sec is shown on Fig. 11.

(b) The Kay Lab Notch Filter (cathode followers included)

Fig. 11 shows the theoretical plot of the transfer function of the notch filter with the attenuation of the two cathode followers included. To establish this plot, a constant, -2.47 db, was substracted from the plot of equation (38).

APPENDIX III

Mathematical evaluation of the cathode follower gain product for the Kay Lab notch filter.

INPUT CATHODE FOLLOWER*	OUTPUT CATHODE FOLLOWER*
$R_k = 11.2\ K\Omega$	$R_k = 9.0\ K\Omega$
$E_{kg} = 40$ volts	$E_k = 52$ volts
$I_{dc} = \frac{E_k}{R_k} = \frac{40}{11,200} = 3.57$ ma	$I_{dc} = \frac{E_k}{R_k} = \frac{52}{9,000} = 5.79$ ma
From RCA Tube Handbook, Vol. 5-6: Characteristic curves for 12AU7:	From RCA Tube Handbook, Vol. 5-6: Characteristic curves for 12AU7:
$r_p = 13.0\ K$	$r_p = 10.5\ K$
$\mu = 13.5$	$\mu = 15.0$
$A_1 = \frac{\mu R_k}{r_p + (1+\mu)R_k}$	$A_2 = \frac{\mu R_k}{r_p + (1+\mu)R_k}$
$= \frac{(13.5)(11,200)}{13,000 + (14.5)(11,200)}$	$= \frac{(15.0)(9,000)}{10,500 + (16.0)(9,000)}$
$= 0.86$	$= 0.873$

$\therefore A_{CF} = A_1 A_2 = (0.86)(0.873) = 0.752 = -2.47db$

*The values of the circuit parameters used to establish the 12AU7 operating points were measured with a vacuum tube voltmeter.